O

OCEAN BOTTOM SEISMICS

Ingo A. Pecher[1,2], Jörg Bialas[3], Ernst R. Flueh[3]
[1]GNS Science, Lower Hutt, New Zealand
[2]Institute of Petroleum Engineering, Heriot-Watt University, Edinburgh, UK
[3]Leibniz-Institut für Meereswissenschaften, University of Kiel, Kiel, Germany

Synonyms

Ocean bottom seismology

Introduction

Ocean bottom seismics, recording of seismic waves on the ocean floor by seismometers placed on the ocean floor, is becoming increasingly common both in academic research surveys and for hydrocarbon exploration. The main advantages of ocean bottom seismics over reflection seismics with hydrophone streamers (see *Seismic Data Acquisition and Processing*) are that the use of receivers on the seafloor yields sufficient source-receiver offsets to analyze the deeper crustal velocity structure, deploying multicomponent receivers allows recording of shear waves, and that instruments can be deployed for an extended time to record natural seismicity. In most cases, the seismic sources are either airguns towed on the sea surface or natural seismicity. Seafloor sources are rare.

Instrumentation

Seismic seafloor receivers fall broadly into three categories, (1) ocean bottom seismometers (OBSs), individual receivers that can be deployed and recovered without the need of any specialized vessels, (2) ocean bottom cables (OBCs), streamer-like arrays of receivers that are deployed from a specialized vessel, and (3) ocean bottom seismic nodes, individual receivers that require underwater vehicles for deployment and retrieval.

Ocean bottom seismometers

OBSs are individual stations that contain sensors and electronics for data storage (Figure 1). These instruments are deployed from a vessel, and descend to the seafloor weighted by an anchor. A release mechanism is activated toward the end of the survey, detaching the instrument from the anchor. The instrument then rises to the surface buoyed by flotation devices. The instrument is recovered onto the vessel where the recorded data are downloaded. The term ocean bottom seismometer is sometimes used for any instrument that records seismic waves at the seafloor, including OBCs and ocean bottom seismic nodes.

Communication with OBSs while on the seafloor is usually performed with acoustic transmission. This includes releasing the instrument from the anchor; although sometimes, a time-based release is used as backup in case communication fails. Acoustic communication is also used for determining the position of the instrument at the seafloor by triangulation and for checking the status of the instrument.

OBSs that contain only a hydrophone as receiver are often called ocean bottom hydrophones. Hydrophones record pressure waves in the water. Some instruments contain vertically oriented geophones, mostly in combination with hydrophones. But, more commonly used OBSs have 3-component geophones (one vertical, two horizontal components) or 4-component (4-C) OBSs that contain 3-component geophones and a hydrophone. The type of geophone varies, depending on application – usually 4.5 Hz geophones (geophones with a resonance frequency at 4.5 Hz) for active-source experiments. Broadband seismometers with varying frequency bands (with periods as low as several tens of seconds) are used for recording of natural seismicity. In a few cases, accelerometers

Harsh K. Gupta (ed.), *Encyclopedia of Solid Earth Geophysics*, DOI 10.1007/978-90-481-8702-7,

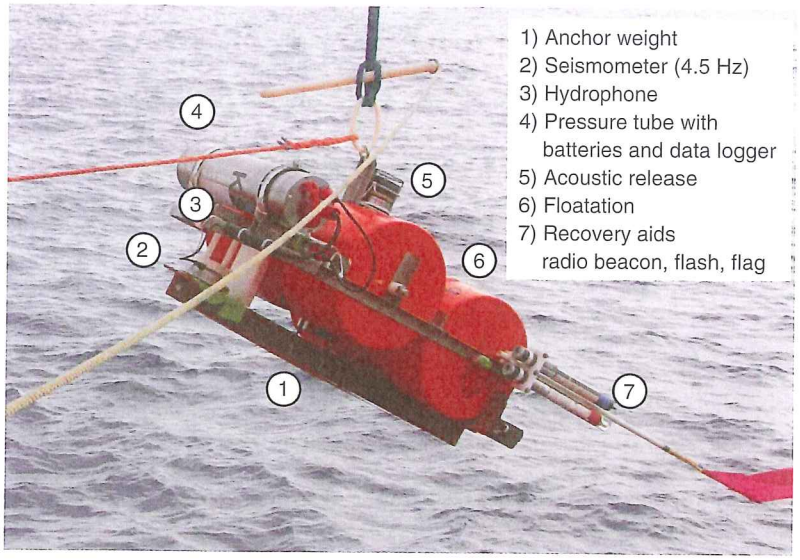

Ocean Bottom Seismics, Figure 1 Ocean bottom seismometer (instruments used by IfM-Geomar, Kiel, Germany).

(measuring particle acceleration rather than velocity as in geophones) are used to record seismic waves.

Seismic data are recorded continuously. Storage media have evolved from analogue tapes to hard drives and flash drives. Exact time stamps from an internal clock are critical for OBS records. GPS time synchronization is completed before and after deployment. Modern high precision clocks keep the deviation as low as 0.05 ppm (4.3 ms/day). For active-source experiments, the records are split into receiver gathers using shot times, usually in SEG-Y format. Data processing varies widely depending on the application and resembles that of land data. Some peculiarities of OBS records include unknown receiver locations, unknown orientations of the horizontal components, and a lack of continuous GPS time stamps. Typical specifications of a modern OBS are listed in Table 1.

Until the 1990s active-source OBS surveys typically involved 10–50 OBSs deployed along a seismic transect. Spacing between instruments for a survey targeting the deeper crustal structure typically was between 5 and 20 km, allowing traveltime analysis of wide-angle reflected and refracted arrivals. In the past decade, significant improvements in hardware and electronics have made instruments less expensive and shortened turnaround times. This has led to a number of experiments with considerably more OBSs allowing imaging of deep crustal structures and 3D traveltime analysis (e.g., Kodaira et al., 2000; Morgan et al., 2002).

Advances in batteries and storage devices also make it possible to continuously record seismicity with OBSs for up to ~1 year. The use of additional batteries may extend this time window but even for frames and housing made of titanium, corrosion is a problem. Therefore a service recovery after ~1 year is good practice. Such passive-source experiments are becoming more common to study the earth's deep structure, subduction zones on regional scales, as well as seismically active local features such as mud volcanoes (Brueckmann et al., 2009). A combination of onshore and offshore seismological networks has shown to significantly improve the determination of near-shore hypocenters (Husen et al., 1999; Arroyo et al., 2009).

Ocean Bottom Seismics, Table 1 Specification of modern OBS

Recording channels	Min. 4 (hydrophone, 3-component seismometer) Optional additional channels for supplementary sensors (e.g., pressure, CH_4, temperature)
Sampling rate	20 Hz to 1 kHz (passive or active seismology)
Data capacity	Tens of GB with flash memory (lowest power) >50 GB with low power disk drives
Time stability	GPS synchronized prior and after mission Timing accuracy 0.05 ppm/0.03 ppm (2.6/4.3 ms/day; depending on power consumption)
Resolution	20 + bit, 32 bit ideally wanted (not yet available)
Power consumption	<250 mW when active (depending on sensors)
Time of operation	Depending on battery supply up to 1 year
Release system	Acoustic release (optional with additional time release); burn wires, gradually replaced by motor-driven hooks
Recovery aids	Radio beacon, flash light Optional: flag, shroud line

Ocean bottom cables

OBCs are densely spaced receivers attached to a cable. The cable is deployed from a vessel, usually a specialized ship (Figure 2). Seismic data are transmitted along the cable to be recorded on the vessel. Typical receiver spacing is 25 m. Most modern cables are equipped with 4-C receivers. Cables are often dragged

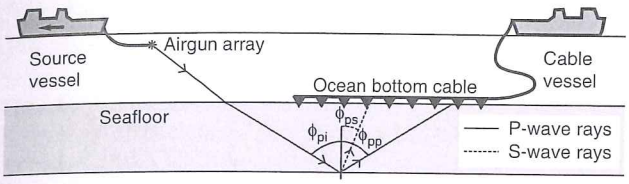

Ocean Bottom Seismics, Figure 2 OBC acquisition. Part of the downgoing P-wave energy is converted upon reflection to upgoing S-wave energy. ϕ_{pi}: angle of incidence, downgoing P-wave. ϕ_{pp}: exit angle, reflected P-wave. ϕ_{ps}: exit angle, P-to-S converted wave. Ray angles according to Snell's Law, that is, $\phi_{pi} = \phi_{pp}$ and $\sin(\phi_{ps})/V_s = \sin(\phi_{pi})/V_p$.

along the seafloor to achieve deployment in a straight line. Some OBCs use geophones that are being pushed into the seafloor by remotely operated vehicles (ROVs) to improve coupling to the seafloor. OBCs may also be deployed in trenches to improve coupling and reduce noise, such as for the Life of Field experiment for long-term monitoring of the Valhall oil field, North Sea (Barkved and Kristiansen, 2005).

OBCs allow imaging of the subsurface with similar coverage as surface-towed streamers. Furthermore, coupling between receivers and seafloor is generally far better than for OBSs partly because the mass of the recording equipment is much smaller, and partly because the deployment techniques for OBCs facilitate slight "burrowing" of cables into the seafloor. OBCs are widely used in the oil and gas exploration industry. The need for a specialized cable deployment vessel, however, normally makes OBCs prohibitively expensive for academic research to date.

Ocean bottom seismic nodes

Ocean bottom seismic nodes are individual receivers with independent recording units – essentially, OBSs without anchors and flotation devices. They are typically deployed with ROVs making their deployment relatively expensive compared to OBSs. Nodes are often deployed to fill coverage gaps in OBC surveys, for example, in the immediate vicinity of platforms where it is unsafe to deploy OBCs (or OBSs). Nodes are often pushed into the seafloor, which potentially leads to improved receiver coupling (Caldwell, 1999).

Ocean bottom seismic sources

By far the majority of active-source OBS surveys use pressure waves generated by airguns towed behind a vessel, although some ocean bottom sources have been pioneered, mainly to generate shear waves.

Explosives have been used as sources at the seafloor for an experiment to record shear waves in boreholes during Ocean Drilling Program Leg 156 but because of the strong increase of shear (S-) wave velocity with depth beneath the seafloor, rays were bent away from the borehole and did not reach borehole receivers (Peacock et al., 1997). Furthermore, environmental and health and safety concerns preclude large-scale use of seafloor explosives.

Imploding glass spheres are the source of the SEEBOSEIS system, for which glass spheres containing air at atmospheric pressure are punctured on the seafloor (Nguyen et al., 2009).

Shear-wave "sleds" are occasionally used to study the high-resolution shear-wave structure of the first few meters beneath the seafloor. One such system uses an electromagnetic coil to generate seismic shear energy at the seafloor. Receivers are dragged along the seafloor behind the source. This system has been used successfully, for example, to measure near-seafloor S-wave velocity offshore California (Huws et al., 2000).

Applications

P-waves

OBSs have been used extensively in the last 4 decades to study the crustal structure beneath the seafour (see *Deep Seismic Reflection and Refraction Profiling*) from P-wave traveltime analysis. A typical survey, for example, for a transect across a subduction zone consists of 20+ instruments spaced between 5 and 20 km. Seismic shot lines with maximum offsets of often >100 km are acquired with a large (~4,000–8,000 cu-in = 65–130 l) airgun array. Often, a coincident seismic reflection profile is acquired with the shot vessel although, in order to avoid noise from previous shots to interfere with arrivals from deep targets, shot intervals for crustal OBS surveys should be much larger (~60 s, equivalent to 100–150 m shot spacing) than would be desired for reflection surveying (~15 s) (Christeson et al., 1996) (see *Single and Multichannel Seismics*).

Such a configuration typically allows recording of reflected and refracted arrivals down to the base of the crust as well as refracted waves through the upper mantle (Figure 3). Records are similar to those from land surveys, albeit often at considerably higher signal-to-noise ratio, and receivers and shots are reversed; land crustal wide-angle surveys typically have sparse shot and dense receiver spacing, whereas marine OBS surveys have dense shot but sparse receiver spacing.

Data processing often only involves bandpass filtering and amplitude scaling. Typical sources of noise or data contamination include reverberations particularly on horizontal components, previous-shot noise, water-column multiples, and noise from underwater currents that may shake the instruments.

As for land surveys, data are often displayed using a reduced traveltime ($t_{red} = t - x/v_{red}$, where t_{red}: reduced time, x: source-receiver offset, v_{red}: reduction velocity). The origin of arrivals is identified and their traveltimes are picked, followed by traveltime analysis to determine seismic velocities (see *Traveltime Tomography Using Controlled-Source Seismic Data*). The latter is performed based on ray-trace modeling (e.g., Zelt and Smith, 1992). In the past decade, traveltime inversion has become

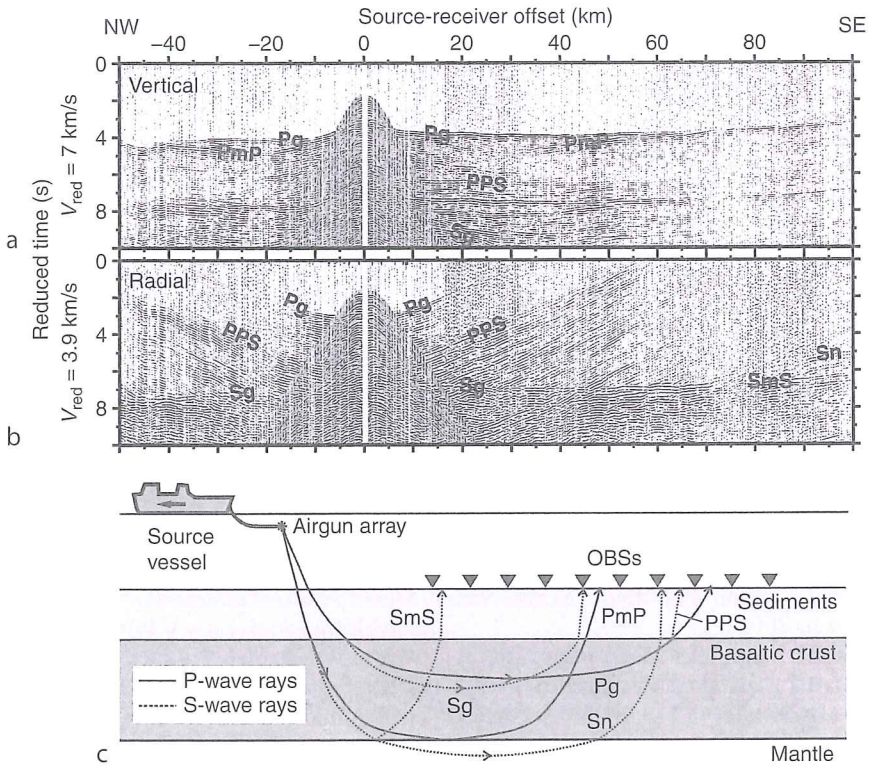

Ocean Bottom Seismics, Figure 3 Example of an OBS record from offshore the Faeroe Islands with interpreted arrivals (after Eccles et al., 2009). (**a**) vertical component, (**b**) rotated radial component, (**c**) schematic ray paths. See text in chapter on converted waves for details on radial component. Reduction velocities 7 km/s for vertical component, 3.9 km/s for radial component. Arrivals P-waves: Pg: diving wave in the crust, PmP: reflection from the top of the mantle (Mohorovičić discontinuity). Converted S-waves: PPS: S-wave, converted upon transmission from upgoing P-wave at basalt-sediment interface. Sg: S-wave, converted upon transmission from downgoing P-wave at basalt-sediment interface and diving as S-wave in the basaltic crust. SmS: S-wave, converted upon transmission from downgoing P-wave at basalt-sediment interface and reflected as S-wave at the top of the mantle. Sn: S-wave, converted upon transmission from downgoing P-wave at basalt-sediment interface and diving as S-wave in the mantle. Courtesy Jennifer Eccles (University of Auckland, New Zealand).

common allowing better determination of the uncertainties and uniqueness of resulting velocity models (e.g., Korenaga et al., 2000). However, the uncertainty from potentially misinterpreting the origin of arrivals is difficult to quantify.

Coincident OBS and seismic reflection surveys are being used for high-resolution studies of the first few hundreds of meters beneath the seafloor, in particular to obtain velocity information in the gas-hydrate zone. Data analysis usually comprises joint analysis of reflected and refracted P-waves often with additional structural information from seismic reflection data (Hobro et al., 1998). Many of these experiments are designed to achieve 3D ray coverage, sometimes coincident with 3D seismic reflection data (Plaza-Faverola et al., 2010). OBS experiments designed for 3D traveltime analysis have also become more common for surveys targeting the deeper crust (e.g., Morgan, et al., 2002).

The increased availability of OBSs has also led to a number of surveys using OBSs with sufficiently dense spacing to allow imaging of deep crustal structures similar to seismic reflection data (e.g., Kodaira, et al., 2000). Advancements in wide-angle migration techniques are key toward successful imaging with OBSs (e.g., Talwani and Zelt, 1998). Imaging using OBSs is also improved by increased reflection coverage by utilizing rays from seafloor multiples, that is, rays that are reflected at the seafloor and sea surface, often referred to as mirror imaging (e.g., Grion et al., 2007).

High-resolution (sub-seismic-wavelength) P-wave velocities have been extracted from OBS data using 1D full-waveform inversion techniques similar to those applied to multichannel reflection data (Korenaga et al., 1997). Increases in computing power now also allow 2D visco-acoustic full-waveform tomography (Sourbier et al., 2009a, b) (see *Seismic, Waveform Modeling and Tomography*).

P-to-S converted waves

Identification of P-to-S converted (PS-) waves in horizontal-component records has led to a paradigm shift in ocean bottom seismics in the late 1990s and early 2000s by the

use of OBCs for multicomponent seismic exploration (Figure 2) (see *Energy Partitioning of Seismic Waves*; *Seismic Data Acquisition and Processing*). P-waves are generated on a shooting vessel. They are partly converted at layer interfaces to S-waves. Upgoing S-waves are then recorded with OBCs or sometimes, densely spaced OBSs. The most prominent PS-arrivals are usually arrivals that are converted from downgoing P-waves upon reflection to upgoing S-waves.

Processing sequences for PS-waves require additional steps compared to conventional P-wave seismic reflection data acquired with surface-towed streamers (Stewart et al., 2002). In particular, processing of PS-waves requires separation of P- and S-waves, a rotation of the horizontal components such that a maximum amount of energy is projected into a single component, the radial component, and various modifications to adjust for the asymmetry of the PS-raypaths. A key step of data analysis is the correlation of P- and PS-events. Once P- and PS-events from the same horizons have been identified, determination of the ratio of P-wave velocity (*Vp*) over S-wave velocity (*Vs*) is straight-forward (e.g., Granli et al., 1999).

Multicomponent PS-wave surveys are being conducted routinely by the exploration industry, chiefly with the following objectives:

Imaging through gas clouds. P-waves are attenuated significantly in gas-bearing layers, whereas S-waves are almost unaffected by gas. Converted-wave surveys often yield superior images of structures in and beneath gas-bearing sediments even though in many cases the downgoing P-wave still has to penetrate gas (Granli et al., 1999).

Fluid discrimination. Reflection strength of PS-waves is only marginally affected by the pore fill (through its effect on density). Therefore, flat spots, oil-water or gas-water contacts at the base of hydrocarbon reservoirs, which generate P-wave reflections, usually do not cause any noticeable PS-reflections (e.g., MacLeod et al., 1999). For the same reason, PS-waves may help establish whether high negative-polarity P-wave reflections (bright spots) are likely to be caused by gas in sediment pores.

Mapping of sand–shale interfaces. Sand and shale layers often have similar *Vp* and density, which leads to low P-wave reflectivity. However, because *Vs* in sands is usually considerably higher than in shales, sand–shale interfaces often cause strong P-to-S conversion and have been imaged successfully with PS-waves (e.g., MacLeod et al., 1999).

Lithology from Vp/Vs. *Vp* – *Vp/Vs* crossplots may be employed to delineate between sands and shales and to constrain the shale content of reservoir sands (Margrave et al., 1998). *Vp/Vs* may also allow to distinguish between different types of carbonates (Rafavich et al., 1984).

Fracture detection from shear-wave splitting. Near-vertical fractures common, for example, in carbonate reservoirs, causes an azimuthal dependence of velocities, azimuthal anisotropy (see *Seismic Anisotropy*). The propagation of S-waves that are polarized perpendicularly to fractures is slower than that of S-waves polarized parallelly to fractures. This leads to PS-waves being split into fast and slow waves, depending on the azimuth of the incoming P-wave, and allows determination of azimuth and magnitude of anisotropy, from which fracture orientation can be inferred (Gaiser et al., 2002).

In recent years, P-to-S converted waves have been utilized increasingly to study *Vs* in the Earth's crust (e.g., Eccles et al., 2009). Unlike for hydrocarbon exploration, with the aim of imaging the sedimentary section with S-waves converted from P-waves upon reflection, studies of the deeper crust often analyze traveltimes of S-waves converted from downgoing P-waves upon transmission. The sediment-basalt interface on the North Atlantic margin between the UK and Iceland, for example, provided a conversion horizon to allow determination of *Vs* in the deeper crust (Figure 3). *Vp* – *Vp/Vs* crossplots allowed lithological conclusions indicating mixing between continental crust and mafic intrusions across the ocean-continent transition and the presence of sub-basalt sediments on the Faeroe Margin (Eccles et al., 2009).

Wide-aperture (wide-azimuth) studies

Wide-aperture studies are increasingly conducted in the hydrocarbon exploration for "undershooting" in order to illuminate the subsurface beneath features that are difficult to penetrate with seismic energy and/or exhibit prominent localized velocity anomalies, such as gas clouds or salt domes: Rays in wide-aperture surveys may bypass these features and reach deeper targets of interest. The length of seismic streamers towed behind the same vessel that tows the airgun sources may not be sufficient for wide-aperture studies. Seismic arrivals at wide apertures may be recorded with surface-towed streamers by using separate vessels for sources and receivers. Alternatively, receivers deployed at the seafloor may be used. An acquisition campaign partly aimed at obtaining wide-aperture data across the Atlantis Field in the deep-water Gulf of Mexico involved 900 ocean bottom seismic nodes (Barley and Summers, 2007). 3D surveys with ocean bottom receivers also provide illumination of seismic targets from different azimuths (multi-azimuth surveys), which allows analysis for azimuthal anisotropy and may improve image quality. Wide-aperture seismic in the hydrocarbon exploration industry is often acquired as part of "seismic-on-demand" 4D surveys over permanently installed seismic surveillance systems such as at the Valhall Field (Barley and Summers, 2007 and references therein).

Passive-source seismology

The use of modern storage media has led to a decrease in power consumption and an increase of storage capacity allowing deployments of OBSs for several months to over

a year to record natural seismicity (Figure 4). Because of the lower frequencies of natural seismic sources usually, broadband geophones are used with a lower resonance frequency than the 4.5 Hz geophones typically used for active-source surveys. Both local seismicity and teleseismic events are being evaluated similarly to data from land-seismic records. Unlike for land data, however, receiver location and geophone orientation need to be established. Local noise conditions in the deep oceans vary significantly throughout the seasons, but in general, noise is higher than on well-placed land stations. In addition, the seismic waveforms are contaminated by water-column multiples.

A very different application of passive-source ocean bottom seismology is to measure seafloor compliance. Pressure variations from ocean waves (gravity or infragravity waves) are being transmitted into the seafloor. Seafloor compliance is the transfer function between pressure loading and seafloor deformation. This transfer function is determined as a function of frequency and depends largely on the subsurface shear modulus (Crawford et al., 1991). Pressure variations are typically recorded with differential pressure gauges, seafloor deformation derived from acceleration measured with self-leveling gravimeters. The frequency range of the analyzed pressure variations depends largely on water depth – because of the dispersion of ocean-surface waves, short-period waves are not transmitted into deeper waters. The resolution of subsurface shear-modulus analyses from compliance measurements decreases with decreasing frequencies. As an example, the frequency range for studying gas-hydrate-bearing sediments at 1.3 km water depth and 2 km beneath the seafloor was 0.003–0.049 Hz (Willoughby et al., 2008).

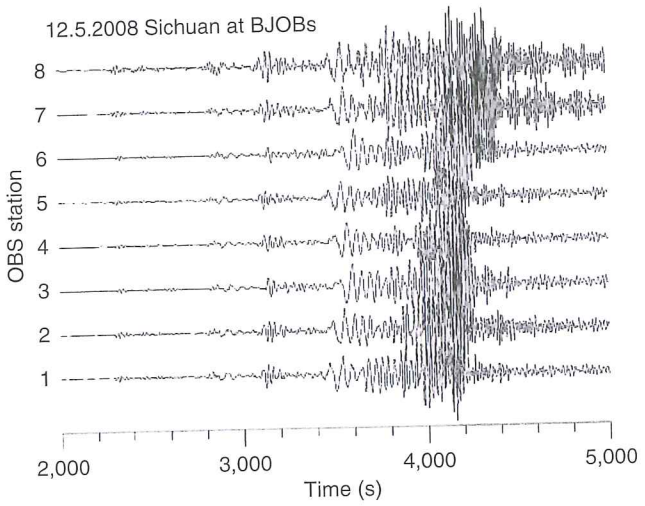

Ocean Bottom Seismics, Figure 4 Teleseismic event on array of broadband OBSs at ~74°N 17°E (between Norway and Spitsbergen), the Mw 7.9 Sichuan Earthquake (China), May 12, 2008. Courtesy Frank Krüger (University of Potsdam, Germany).

Future developments

One of the most significant challenges for autonomous OBSs is still the power supply. Both data loggers and storage media are becoming increasingly energy efficient. Together with new battery technology and further improvement of fuel cells, this is leading to reduction of weight and size of instrumentation. Some study areas may provide additional power sources, such as thermal energy. Weight and size reduction in modern instruments is achieved in most cases by installing all the components in a single glass sphere. On the other hand, glass spheres require increased service efforts and precautions compared to more robust, but larger and heavier titanium pressure casing.

The use of ocean bottom sensors in permanent ocean-floor observatories is likely to become more common. OBSs have already been installed for long-term monitoring at seafloor observatories (e.g., GEOSTAR, Beranzoli et al., 2003) and have been integrated in deployments for tsunami warning systems. These observatories generally have the capability of data transmission to shore. Regional studies usually require a deployment of an array of sensors distributed over an area of several square kilometers. Several seismic seafloor observatories have been established to study the seismogenic zone offshore of Japan and a network of 20 instruments is being developed as part of the Japanese Dense Oceanfloor Network System for Earthquakes and Tsunamis (Kaneda et al., 2009).

Combined seismic and electromagnetic field experiments are becoming more common as the combination of both methods is proving powerful for studying subsurface lithology (Constable and Srnka, 2007 and references therein). Despite significant technical challenges, especially with contamination of electromagnetic signals from the seismic instrumentation, it is conceivable that future ocean bottom instruments will include sensors for both seismic and electromagnetic waves.

The use of OBCs and nodes for hydrocarbon exploration and field appraisal appears to have become a "mainstream" technique. While costs for deployments of either type of instruments are still high compared to conventional 3D streamer seismic, they need to be weighed against the risk of mispositioning considerably more expensive appraisal wells (Barley and Summers, 2007). Furthermore, several hydrocarbon fields are now being monitored with permanent installation of ocean bottom sensors for repeat-seismic surveys in order to guide field development (Barley and Summers, 2007 and references therein).

Conclusions

The last decade has seen a substantial increase of ocean bottom seismic studies. While seafloor seismic sources are rarely deployed, the use of seafloor seismic sensors has established itself primarily for recording offshore wide-angle data, P-to-S converted waves, and natural seismicity. Academic research surveys, for studying the

deeper crustal structure, are usually conducted with autonomous OBSs, which are relatively inexpensive and versatile. Surveys by the exploration industry for evaluating and developing hydrocarbon reservoirs mostly involve deployment of ocean bottom cables or ocean bottom seismic nodes, which give superior data quality compared to OBSs but at much higher cost. In recent years, permanent deployment of instruments has become more common in ocean bottom observatories and for monitoring the development of hydrocarbon fields. The rapid development of ocean bottom seismic instruments is leading to improvements in reliability, data quality, and efficiency, which makes it likely that ocean bottom seismics will continue to expand significantly in the future.

Acknowledgments

We would like to thank Stuart Henrys (GNS Science) and an anonymous external reviewer for constructive comments. We also thank Jennifer Eccles (University of Auckland, New Zealand) and Frank Krüger (University of Potsdam, Germany) for providing the images in Figures 3 and 4, respectively.

Bibliography

Arroyo, I. G., Husen, S., Flueh, E. R., Gossler, J., Kissling, E., and Alvarado, G. E., 2009. Three-dimensional P-wave velocity structure on the shallow part of the Central Costa Rican Pacific margin from local earthquake tomography using off- and onshore networks. *Geophysical Journal International*, **179**, 827–849.

Barkved, O. I., and Kristiansen, T., 2005. Seismic time-lapse effects and stress changes: examples from a compacting reservoir. *The Leading Edge*, **24**, 1244–1248.

Barley, B., and Summers, T., 2007. Multi-azimuth and wide-azimuth seismic: shallow to deep water, exploration to production. *The Leading Edge*, **26**, 450–457.

Beranzoli, L., Braun, T., Calcara, M., Casale, P., DeSantis, A., D'Anna, G., DiMauro, D. G. E., Favali, P., Fuda, J.-L., Frugoni, F., Gamberi, F., Marani, M., Millot, C., Montuori, C., and Smriglio, G., 2003. Mission results from the first GEOSTAR observatory (AdriaticSea, 1998). *Earth Planets Space*, **55**, 361–373.

Brueckmann, W., Tyron, M. D., Bialas, J., Feseker, T., and Lefeldt, M. R., 2009. Monitoring the dynamic properties of an active Mud Volcano in the West Nile Delta. *Eos Transactions AGU*, 90, Fall meeting supplement, Abstract OS21A-1156.

Caldwell, J., 1999. Marine multicomponent seismology. *The Leading Edge*, **18**, 1274–1282.

Christeson, G. L., Nakamura, Y., McIntosh, K. D., and Stoffa, P. L., 1996. Effect of shot interval on ocean bottom seismograph and hydrophone data. *Geophysical Research Letters*, **23**, 3783–3786.

Constable, S., and Srnka, L. J., 2007. Special section – marine controlled-source electromagnetic methods: an introduction to marine controlled-source electromagnetic methods for hydrocarbon exploration. *Geophysics*, **72**, WA3–WA12.

Crawford, W. C., Webb, S. C., and Hildebrand, J. A., 1991. Seafloor compliance observed by long-period pressure and displacement measurements. *Journal of Geophysical Research*, **96**(B), 16151–16160.

Eccles, J. D., White, R. S., and Christie, P. A. F., 2009. Identification and inversion of converted shear waves: case studies from the European North Atlantic continental margins. *Geophysical Journal International*, **179**, 381–400.

Gaiser, J., Loinger, E., Lynn, H., and Vetri, L., 2002. Birefringence analysis at Emilio Field for fracture characterization. *First Break*, **20**, 505–514.

Granli, J. R., Arntsen, B., Sollid, A., and Hilde, E., 1999. Imaging through gas-filled sediments using marine shear-wave data. *Geophysics*, **64**, 668–677.

Grion, S., Exley, R., Manin, M., Miao, X.-G., Pica, A., Wang, Y., Granger, P.-Y., and Ronen, S., 2007. Mirror imaging of OBS data. *First Break*, **25**, 37–42.

Hobro, J. W. D., Minshull, T. A., and Singh, S. C., 1998. Tomographic seismic studies of the methane hydrate stability zone in the Cascadia margin. In Henriet, J. P., and Mienert, J. (eds.), *Gas Hydrates; Relevance to World Margin Stability and Climatic Change*. Geological Society of London Special Publication, 137. London: Geological Society, pp. 133–140.

Husen, S., Kissling, E., Flueh, E., and Asch, G., 1999. Accurate hypocentre determination in the seismogenic zone of the subducting Nazca Plate in northern Chile using a combined on-/offshore network. *Geophysical Journal International*, **138**, 687–701.

Huws, D. G., Davis, A. M., and Pyrah, J. R., 2000. A Nondestructive Technique for Predicting the In Situ Void Ratio for Marine Sediments. *Marine Georesources and Geotechnology*, **18**, 333–346.

Kaneda, Y., Kawaguchi, K., Araki, E., Sakuma, A., Matsumoto, H., Nakamura, T., Kamiya, S., Ariyoshi, K., Baba, T., Ohori, M., and Hori, T., 2009. Dense Ocean floor Network for Earthquakes and Tsunamis (DONET) – development and data application for the mega thrust earthquakes around the Nankai trough. *Eos Transactions AGU*, 90, Fall meeting supplement, Abstract S53A-1453.

Kodaira, S., Takahashi, N., Kato, A., Park, J.-O., Iwasaki, T., and Kaneda, Y., 2000. High pore fluid pressure may cause silent slip in the NankaiTrough. *Science*, **308**, 1295–1298.

Korenaga, J., Holbrook, W. S., Singh, S. C., and Minshull, T. A., 1997. Natural gas hydrates on the southeast US margin: constraints from full waveform inversion and traveltime inversion of wide-angle seismic data. *Journal of Geophysical Research*, **102**(B), 15345–15365.

Korenaga, J., Holbrook, W. S., Kent, G. M., Kelemen, P. B., Detrick, R. S., Larsen, H. C., Hopper, J. R., and Dahl-Jensen, T., 2000. Crustal structure of the southeast Greenland margin from joint refraction and reflection seismic tomography. *Journal of Geophysical Research*, **105**(B), 21,591–21,614.

MacLeod, M. K., Hanson, R. A., and Bell, C. R., 1999. The Alba field ocean bottom cable seismic survey: impact on development. *The Leading Edge*, **18**, 1306–1312.

Margrave, G. F., Lawton, D. C., and Stewart, R. R., 1998. Interpreting channel sands with 3C-3D seismic data. *The Leading Edge*, **17**, 509–513.

Morgan, J. V., Christeson, G. L., and Zelt, C. A., 2002. Testing the resolution of a 3D velocity tomogram across the Chicxulub crater. *Tectonophysics*, **355**, 215–226.

Nguyen, X. N., Dahm, T., and Grevemeyer, I., 2009. Inversion of Scholte wave dispersion and waveform modeling for shallow structure of the Ninetyeast Ridge. *Journal of Seismology*, **13**, 543–559.

Peacock, S., Westbrook, G. K., and Graham, D. P., 1997. Seismic velocities in the Northern Barbados Ridge accretionary comples, Site 949. In Shipley, T. H., Ogawa, Y., Blum, P., and Bahr, J. M. (eds.), *Proceedings ODP, Scientific Results: Ocean Drilling Program*, Vol. 156, pp. 263–275.

Plaza-Faverola, A., Bünz, S., and Mienert, J., 2010. Fluid distributions inferred from P-wave velocity and reflection seismic amplitude anomalies beneath the Nyegga pockmark field of the mid-Norwegian margin. *Marine and Petroleum Geology*, **27**, 46–60.

Rafavich, F., Kendall, C. H. S. C., and Todd, T. P., 1984. The relationship between acoustic propertoes and the petrographic character of carbonate rocks. *Geophysics*, **49**, 1622–1636.
Sourbier, F., Operto, S., Virieux, J., Amestoy, P., and L'Excellent, J.-Y., 2009a. FWT2D: a massively parallel program for frequency-domain full-waveform tomography of wide-aperture seismic data – part 1 algorithm. *Computers and Geosciences*, **35**, 487–495.
Sourbier, F., Operto, S., Virieux, J., Amestoy, P., and L'Excellent, J.-Y., 2009b. FWT2D: a massively parallel program for frequency-domain full-waveform tomography of wide-aperture seismic data – part 2 numerical examples and scalability analysis. *Computers and Geosciences*, **35**, 496–514.
Stewart, R. S., Gaiser, J. E., Brown, R. J., and Lawton, D. C., 2002. Converted-wave seismic exploration: methods. *Geophysics*, **67**, 1348–1363.
Talwani, M., and Zelt, B., 1998. Some recent developments in the acquisition and processing of seismic data. *Tectonophysics*, **286**, 123–142.
Willoughby, E. C., Latychev, K., Edwards, R. N., Schwalenberg, K., and Hyndman, R. D., 2008. Seafloor compliance imaging of marine gas hydrate deposits and cold vent structures. *Journal of Geophysical Research*, **113**, B07107.
Zelt, C. A., and Smith, R. B., 1992. Seismic traveltime inversion for 2-D crustal velocity structure. *Geophysical Journal International*, **108**, 16–34.

Cross-references

Deep Seismic Reflection and Refraction Profiling
Energy Partitioning of Seismic Waves
Seismic Anisotropy
Seismic Data Acquisition and Processing
Seismic, Waveform Modeling and Tomography
Single and Multichannel Seismics
Traveltime Tomography Using Controlled-Source Seismic Data

OCEAN, SPREADING CENTRE

K. S. Krishna
Geological Oceanography, National Institute of Oceanography (Council of Scientific and Industrial Research), Dona Paula, Goa, India

Definition

The *oceanic spreading center*, also known as the midocean ridge, is an underwater mountainous feature lying between the two lithospheric plates, through which new magma material being continuously spread out and lead to growth of the lithospheric plates.

Ridge structure, partial melted mantle upwelled through the midocean ridge, forms a 3–6 km thick basaltic crust, but at a later stage the same crust moves away from the ridge crest and allows growth of mantle component.

Introduction

The rigid surface layer (generally about 70–100 km thick) of the Earth comprising the crust and uppermost mantle, *termed as lithosphere*, is divided into a number of tectonic plates. Presently, there are about eight primary plates, namely, North American, South American, African, Indian, Australian, Antarctica, Eurasian, and Pacific; seven secondary plates; and several more tertiary plates covering the Earth's surface (for details, see wikipedia web site: http://en.wikipedia.org/wiki/List_of_tectonic_plates). The lithospheric plates are bounded by one of the three main types of geological features: (1) midoceanic ridges, (2) subduction zones, and (3) transform faults. The boundaries are narrow deforming zones and are associated with intense seismicity, whereas the plate's interiors are relatively stable. The plates upon which continents and ocean floor lie are in continuous motion at a speed of few centimeters per year. Each plate is in relative motion with respect to the other on the surface of the Earth. The relative motion produces new crust at midoceanic ridges and consumes old lithosphere at subduction zones. Apart from these tectonic processes, plates do undergo breakups and unifications through geologic time.

Morphology and spreading rates of midoceanic ridge

A midocean ridge is an underwater linear physiographic feature and serves as a divergent tectonic boundary between two lithospheric plates. The midocean ridges, those encircle the entire globe, are physically connected and extend for a total length of about 65,000 km as a single global entity in the world oceans (Figure 1). Many of the major oceanic ridges in the world oceans have been reconfigured in the geological past that led to unification and split of the lithospheric plates. One of the well-mapped ancient oceanic ridges in the Indian Ocean is the Wharton Ridge, once separated the Indian and Australian plates, and the ridge cessation at about 42 million years ago led to unification of both the aforesaid plates into a single Indo-Australian plate (Liu et al., 1983; Krishna et al., 1995).

On the ocean floor, long, linear, and elevated features are observed with variable seafloor undulations (Figure 2). They are the places where magma is continuously upwelling and being added to the previously formed oceanic crust on either side. The upwelling magma rates along the global midoceanic ridges are not fixed; they greatly vary with a range from 6 to 200 mm/year. Following the seafloor expansion rates, the midoceanic ridges are classified into categories of slow, intermediate, and fast spreading ridges. The Gakkel midoceanic ridge located in the Arctic Ocean between Greenland and Siberia (Figure 1) is the slowest spreading ridge with an upwelling magma rate of about 6 mm/year. On the other hand, the East Pacific Rise particularly in equatorial zone generates magma at the fastest rates up to 200 mm/year. The seafloor morphology on the flanks of the midoceanic ridge is largely controlled by the rate of seafloor expansions. Fast expansion spreading rates contribute to generally smooth and flat seafloor surfaces in the vicinity of the ridge, while the slow expansion spreading rates add exceptionally